Mechanics and Mechanical Engineering
Vol. 21, No. 4 (2017) 935–951

Evaluation of Fatigue Life Calculation Algorithm of the Multiaxial Stress–Based Concept Applied to S355 Steel under Bending and Torsion

Wojciech Macek
Norbert Mucha

Opole University of Technology
Faculty of Production Engineering and Logistics
31 Sosnkowskiego Street, 45-272 Opole, Poland
wojciech.macek@yahoo.com

Received (22 July 2017)
Revised (9 August 2017)
Accepted (13 September 2017)

This paper presents the results of a study into the stress-based fatigue life calculation algorithm applied to cyclic and random multiaxial proportional and non-proportional loading. This method for high-cycle fatigue, covers both infinite and finite life region, and is based on a critical plane approach combined with rain flow cycle counting and linear damage accumulation. Algorithm based on the method for equivalent scaling of the normal stress in material planes in dependence on the stress state, proposed by Gaier and Danbauer. For analysis the calculated fatigue lives are compared to the experimental results for steel S355 under proportional and non-proportional bending with torsion.

Keywords: critical plane, stress-based criteria, fatigue life, fatigue damage, multiaxial loading.

1. Introduction

Multiaxial nature of applied stresses causes the fatigue life analysis and calculation to be more complicated. In the algorithms for calculating the fatigue life of structural materials under multiaxial service loading [1-4] a very important role have the procedures for reduction of triaxial stress state to equivalent uniaxial state, which is followed by the cycle count from the strain history, most often using the "rain flow" method [5] and by damage accumulation, according to the accepted hypothesis.
The criteria for assessing the fatigue life can be divided into: stress σ [6-8], strain ϵ [9] and energy parameter [10-12] (stress-strain). In stress-based criteria of multiaxial fatigue, by means of which equivalent stress is determined, stands out models based on stress in critical plane [13-16].
The objective of this work was to verify the algorithm for calculating fatigue life

based on stress on a critical plane approach, compared with fatigue tests [14, 17] obtained at the Department of Mechanics and Machine Design of Opole University of Technology. The character of the algorithm proposed by Gaier and Dannbauer [18, 19], based on the method for equivalent scaling of the normal stress in material planes in dependence on the stress state, is used to calculate the fatigue life of automotive crankshafts subjected to non-proportional [20-23] bending and torsion [24, 25]. The method was analyzed in cyclic non-proportional, quasi-cyclic, and variable amplitude load conditions. It is assumed that in the general case bending and torsion stress state occurs in the material when it is described by two components: normal stress σ originating from the bending and shear stress τ originating from torsion. The value of the stress is not constant in each of the section but varies and depends on the position of this point (Fig. 1). The maximum values of the stresses occur at the points farthest from the longitudinal axis.

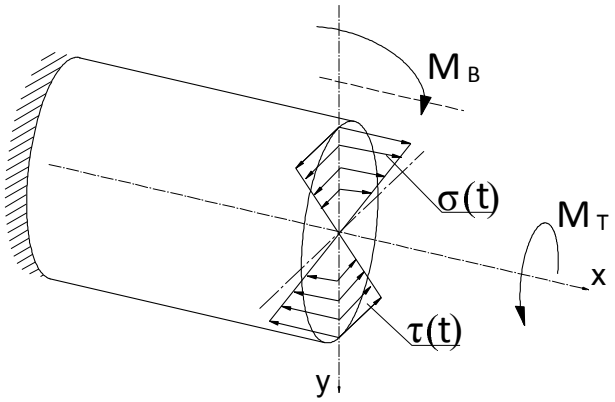

Figure 1 Distribution of normal and shear stress in cross-section of the bending and torsion element

2. Experimental data

Experimental data demonstrate the effect of different values of normal and shear stresses and their correlation for the fatigue life of the selected material, and they were carefully selected in order to verify the efficiency of the verified algorithm. Construction material, which was used for fatigue testing on the basis of which the verification algorithm for calculating the fatigue life was steel S355 [14, 17, 26]. In the Tabs. 1, 2 is presented chemical composition, and static and fatigue strength properties of S355 steel.

Table 1 Chemical composition of S355 steel (wt.%)

C	Mn	Si	P	S	Cr	Ni	Cu	Fe
0.21	1.46	0.42	0.019	0.046	0.09	0.04	0.17	rest

Table 2 Static and fatigue strength properties of S355 steel

R_e MPa	R_m MPa	Z_{RC} MPa	N_{0R} cycle	Z_G MPa	N_{0G} Cycle	A_{10} %	Z %	E GPa	ν
357	535	204	1.12 10^6	270	2.375 10^6	21	50	210	0.30
σ_f' MPa	ϵ'$_f$	m_{RC}		m_G		B	C	n'	K' MPa
782	0.693	8.2		7.17		-0.118	-0.41	0.287	869

The applied S–N fatigue characteristics were determined according to the ASTM standards [27].
Calculations were performed for:
– Sinusoidal non-proportional loadings with phase shift δ equal to $\pi/2$, with different ratios of amplitudes shear stress to normal stress $\lambda_\sigma = \tau_a/\sigma_a$,
– Random loading and three correlation coefficients between bending moment and torsion moments ($r_{\sigma\tau}$ = 0, 0.5, 1.0) and varying the standard deviations of these loadings,
– Quasi–cyclic loadings,
– Variable amplitude loadings with ratios of amplitudes shear stress to normal stress $\lambda_\sigma = \tau_a/\sigma_a$ = 1.0, 0.5, and cross-correlation coefficients $r_{\sigma\tau}$ = 1.0, 0.

2.1. *Random loading*

Calculations for random loads performed for three values of the cross-correlation coefficient $r_{\sigma\tau}$ = 0; 0.5; 1 between the bending moments and torsional moments as well as for different values of the standard deviations of these histories. Using a random number generator, which is available in Matlab software there were generated two histories with a wide frequency band with duration of 33 minutes and 20 seconds, and then subjected to filtration narrowband filter to obtain the dominant frequency f = 20Hz. Figure 2 shows the random course of normal stresses in time σ(t), and shear stresses in time τ(t).

2.2. *Cyclic non-proportional loadings (phase shift δ equal to $\pi/2$)*

Calculation using the cyclic non-proportional loadings were performed for different combinations of ratios of shear stress amplitudes to normal stress $\lambda_\sigma = \tau_a/\sigma_a$ with loading frequency f = 20Hz.

2.3. *Quasi-cyclic loadings*

Calculations under quasi-cyclic bending and torsion included several loading combinations for different combinations of ratios of maximum shear stress to maximum normal stress $\lambda_\sigma = \tau_{max}/\sigma_{max}$. Courses of fatigue loadings characterized by cross-correlation coefficient between normal stresses and shear stresses $r_{\sigma\tau}$ = 0.16, coeficients of irregularity I_σ = 0.99 for bending and I_τ = 0.97 for torsion. Fig. 3 shows the quasi-cyclic course of normal stresses in time σ(t), and shear stresses in time τ(t).

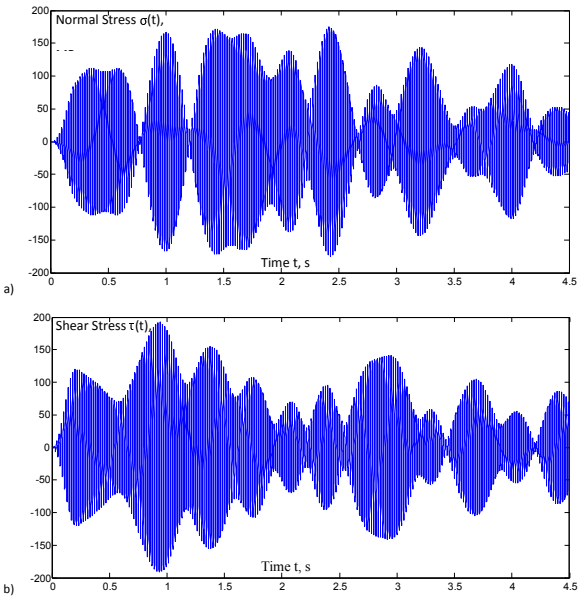

Figure 2 The random course of nominal stresses in time: a) normal stresses σ(t) and b) shear stresses τ(t)

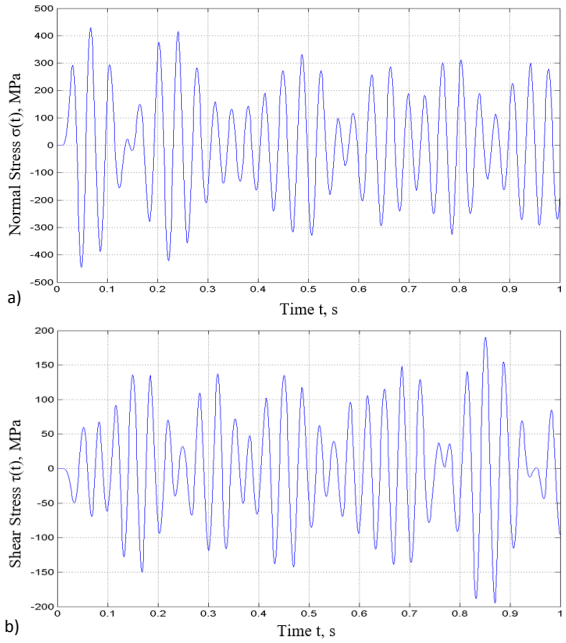

Figure 3 The quasi-cyclic course of nominal stresses in time: a) normal stresses σ(t) and b) shear stresses τ(t)

2.4. *Variable amplitude loadings*

Tests were performed for variable amplitude combination of bending with torsion for two ratios of amplitudes shear stress to normal stress $\lambda_\sigma = 0.5$ and 1 and for three values of the cross-correlation coefficient $r_{\sigma\tau} = 0$, 0.5 and 1. Fig. 4 shows the exemplary variable amplitude courses of normal stresses in time σ(t), and shear stresses in time τ(t), for ratios of shear stress amplitudes to normal stress λ_σ equal to 1.

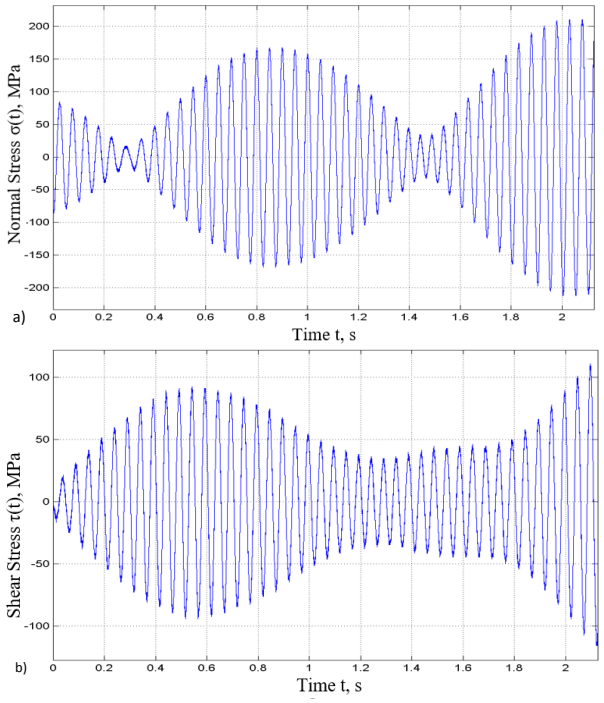

Figure 4 The variable amplitude course of nominal stresses in time: a) normal stresses σ(t) and b) shear stresses τ(t), for $\lambda_\sigma = 1$

3. Description of the applied algorithm

In algorithms for calculating the fatigue life of structural materials subjected to the multiaxial service loadings, a very important role have procedures for reducing the multiaxial stress state to the equivalent uniaxial state of stress. In the group of stress criteria of multiaxial fatigue, by which the equivalent stress is determined, are distinguished the models based on the stress in the critical plane of material [13-16].

In the case of multiaxial loadings, fatigue life is calculated using the algorithm shown in Fig. 5.

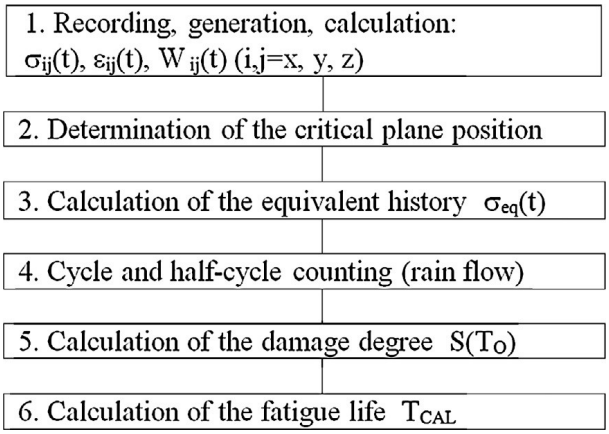

Figure 5 Algorithm of fatigue life assessment for critical plane approach

3.1. *Determination of the critical plane*

The idea to combine the normal and shear stresses in a fixed plane within a material was first proposed by Stanfield [6]. A review of critical plane orientations in multiaxial fatigue failure criteria for metallic materials is provided in [13]. Critical plane position for a given material is dependent on the stress σ, cross-correlation coefficient between normal stresses and shear stresses $r_{\sigma\tau}$ and from ratios of amplitudes shear stress (shear stress amplitudes) to normal stress λ_σ. Using mathematical relationships, the obtained results are not always only one position value of critical plane. Furthermore, the material is never perfect, and damage can occur at the site of the heterogeneity of its structure. According to the adopted method of damage accumulation, the critical plane position is determined by the maximum value of the damage.

In the second block of algorithm of fatigue life assessment for critical plane approach is shown in Fig. 5, followed by positioning of the critical plane. For the planar stress state, the critical plane can be determined using one angle of the plane of the axis of symmetry. The search angles in a critical plane is carried out in the range from -90° to 90° increments 0.5°

3.2. *Calculation of the equivalent stress history*

The combination of bending and torsion loadings induces the planar stress state in a cross-section of the specimen. For test results, set in the Cartesian coordinates σ_a – τ_a, fatigue limit can be approximated by equations (1) and (2).

For ductile material the fatigue limit forms are an ellipse in the normal/shear stress diagram for combined in-phase bending–torsion loading, proposed by Gough

and Pollard [7]:

$$\left(\frac{\sigma_a}{\sigma_{af}}\right)^2 + \left(\frac{\tau_a}{\tau_{af}}\right)^2 = 1 \tag{1}$$

Findley [25] proposed a criterion for brittle material based on the linear combination of the axial stress and the shear stress squared. As a parabola in the normal/shear stress diagram takes the following form:

$$\frac{\sigma_a}{\sigma_{af}} + \left(\frac{\tau_a}{\tau_{af}}\right)^2 = 1 \tag{2}$$

Then, the formulas (1) and (2) can be expressed by the empirical formula:

$$\left(\frac{\sigma_a}{\sigma_{af}}\right)^k + \left(\frac{\tau_a}{\tau_{af}}\right)^2 = 1 \tag{3}$$

where k is the ratio bending to torsion fatigue limit:

$$k = \frac{\sigma_{af}}{\tau_{af}} \tag{4}$$

For brittle materials, we take k equal to 1, and for plastic materials k is 2.
By a linear combination of equations (1) and (2) is replaced by the empirical equation:

$$(k-1)\left(\frac{\tau_a}{\tau_{af}}\right)^2 + (2-k)\left(\frac{\sigma_a}{\sigma_{af}}\right)^k + \left(\frac{\tau_a}{\tau_{af}}\right)^2 = 1 \tag{5}$$

Gaier and Dannbauer proposed a criteria, in which uniaxial equivalent stress history σ_{eq}(t) is scaled by normal stress history σ_n(t):

$$\sigma_{eq}(t) = f(t)\,\sigma_n(t) \tag{6}$$

where $\sigma_n = \sigma_{xx}\cos^2(\alpha) + \tau_{xy}\sin(2\alpha)$ is normal stress, and f(t) is a time-varying magnitude having the following form:

$$f(t) = 1 + (1-k)V(t) \tag{7}$$

This function is dependent on the material, which is expressed by a ratio bending to torsion fatigue limit k according to the relation (4), and from the caused stress state in the material defined by ratio minimum to maximum principal stress:

$$V(t) = \begin{cases} \frac{\sigma_3(t)}{\sigma_1(t)} & \text{for } |\sigma_1(t)| > |\sigma_3(t)| \\ \frac{\sigma_1(t)}{\sigma_3(t)} & \text{for } |\sigma_3(t)| > |\sigma_1(t)| \end{cases} \tag{8}$$

The value of this ratio is in the range from -1 to 1:

- V = -1 for dominating shear stress state,
- V = 0 for dominating normal (tension/compression) stress state,
- V = 1 for hydrostatic stress state.

For brittle material $k = 1$, the stress state will not be modified and variable remains constant $f = 1$, therefore, the equivalent strain is equal to the normal stress. For elasto-plastic materials, the variable f is depends on the state of stress. In the case of tension-compression $V = 0$ equivalent stress is also equal to the normal stress, and in the case of torsion, equivalent stress is a normal stress enlarged by the factor k. For hydrostatic stress states $V = 1$, the factor f will be linearly extrapolated, and the equivalent stress will be decreased to normal stress.
The principal stresses $\sigma_1 > \sigma_2 > \sigma_3$ were calculated according to (9–11):

$$\sigma_1 = \sigma_{xx} + \sqrt{\sigma_{xx}^2 + 4\tau_{xy}^2} \tag{9}$$

$$\sigma_2 = 0 \tag{10}$$

$$\sigma_3 = \sigma_{xx} - \sqrt{\sigma_{xx}^2 + 4\tau_{xy}^2} \tag{11}$$

In order to best fit the computational results of the fatigue life of the experimental results, it is assumed that the ratio k will be variable as a function of number of cycles, and thus:

$$k(N) = \frac{\sigma_a(N)}{\tau_a(N)} \tag{12}$$

where:
$\sigma_a(N)$ – normal stress amplitude versus number of cycles, which can be calculated according to the formula (13),
$\tau_a(N)$ – shear stress amplitude versus number of cycles, which can be calculated according to the formula (14):

$$\sigma_a(N) = \sigma_{af} \left(\frac{N_{fB}}{N} \right)^{\frac{1}{m_\sigma}} \tag{13}$$

$$\tau_a(N) = \tau_{af} \left(\frac{N_{fT}}{N} \right)^{\frac{1}{m_\tau}} \tag{14}$$

in which:
m_σ – regression coefficient for fatigue characteristic under bending,
m_τ – regression coefficient for fatigue characteristic under torsion,
N_{fB} – number of cycles corresponding to fatigue limit σ_{af},
N_{fT} – number of cycles corresponding to fatigue limit τ_{af}.

3.3. *Cycle and half-cycle counting*

In the fourth step of the algorithm of fatigue life assessment for critical plane approach (Fig. 5), the count cycles and half-cycles of the time history of equivalent stress σ_{eq}(t). Cycle counting is used to summarize irregular load-versus-time histories by providing the number of times cycles of various sizes occur. This block applies to random loading, as in the case of cyclic loading the cycle parameters are known. There are known various methods to obtain cycle counts, including level-crossing counting, peak counting, simple-range counting, range-pair counting, and rain?ow counting, which are described in the ASTM standard [5]. Here is used the rainflow-counting algorithm.

3.4. *Calculation of damage degree*

In the fifth step of the algorithm (Fig. 5) the summation of the damage degree for each cycle and half-cycle of time history loading was made. In the case of the applied Palmgren–Miner's linear hypothesis of damage accumulation, based on fatigue characteristics determined by cyclic uniaxial bending:

$$S_{PM}(T_O) = \begin{cases} \sum\limits_{i=1}^{l} \frac{n_i}{N_o \left(\frac{\sigma_{af}}{\sigma_{e,ai}}\right)^m} & \text{for} \quad \sigma_{eq,ai} \geq a\sigma_{af} \\ 0 & \text{for} \quad \sigma_{eq,ai} < a\sigma_{af} \end{cases} \tag{15}$$

where:
$\sigma_{eq,ai}$ – equivalent stress amplitude,
N_0 – the number of cycles corresponding to the fatigue limit σ_{af},
n_i – number of cycles of amplitude $\sigma_{eq,ai}$,
a – factor allows to take into account the amplitude below the fatigue limit in the process of accumulation of fatigue damage (in the paper a=0.5),
l – number of intervals of histogram amplitudes.
Damage accumulation according to Palmgren-Miner's rule, on the basis of the characteristics of bending fatigue, according to the exemplary scheme in Fig. 6.

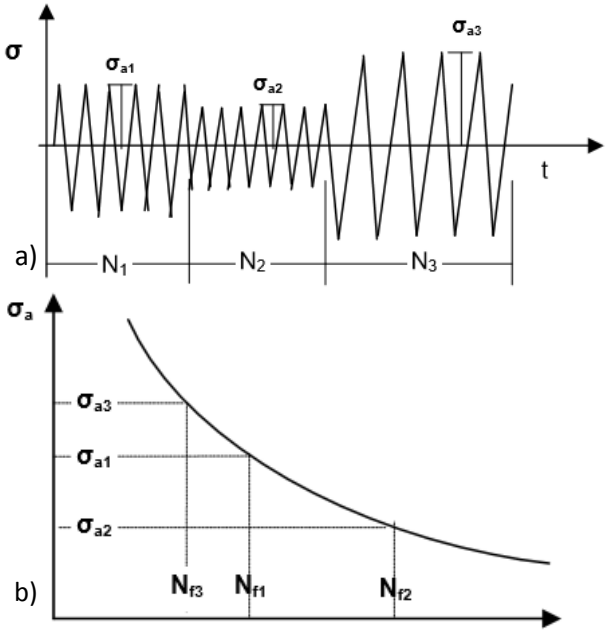

Figure 6 Scheme of use hypothesis Palmgren-Miner to sum of fatigue damage: a) mark for the time history of stress changes, b) signs of Wöhler characteristic

3.5. *Calculation of the fatigue life*

The final step is to calculate the fatigue life of the quotient of the observation period and damage degree $S(\mathrm{T}_0)$:

$$\mathrm{T}_{PM} = \frac{\mathrm{T}_O}{S_{PM}(\mathrm{T}_O)} \tag{16}$$

According to the formula (12), the calculations carried out for the following values of factor k, with corresponding values of number of cycles N:

- $k = 1.7675$ – 1 10^5 cycles,
- $k = 1.6124$ – 5 10^5 cycles,
- $k = 1.5612$ – 1 10^6 cycles,
- $k = 1.5575$ – for fatigue limit,
- $k = 1.4973$ – 2 10^6 cycles.

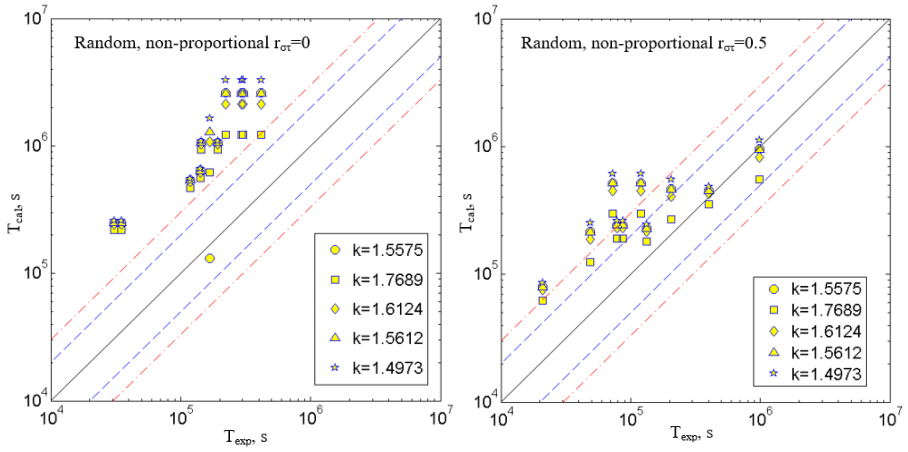

Figure 7 Comparison between experimental T_{exp} and calculated T_{cal} fatigue life for random loadings

4. Results and discussion

Figs. 7–10 present a comparison between the experimental T_{exp} and calculated T_{cal} fatigue lives based on method for equivalent scaling of the stress, proposed by Gaier Danbauer. On charts, the black solid line indicates $\mathrm{T}_{cal} = \mathrm{T}_{exp}$, blue dashed lines correspond to $\mathrm{T}_{cal}/\mathrm{T}_{exp}$ and $\mathrm{T}_{exp}/\mathrm{T}_{cal}$ equal to 2, and the red dash-dot lines correspond to $\mathrm{T}_{cal}/\mathrm{T}_{exp}$ and T_{exp} /T_{cal} equal to 3. Non-conservative results are located above black solid line, and conservative results, respectively, are on lower side of charts.

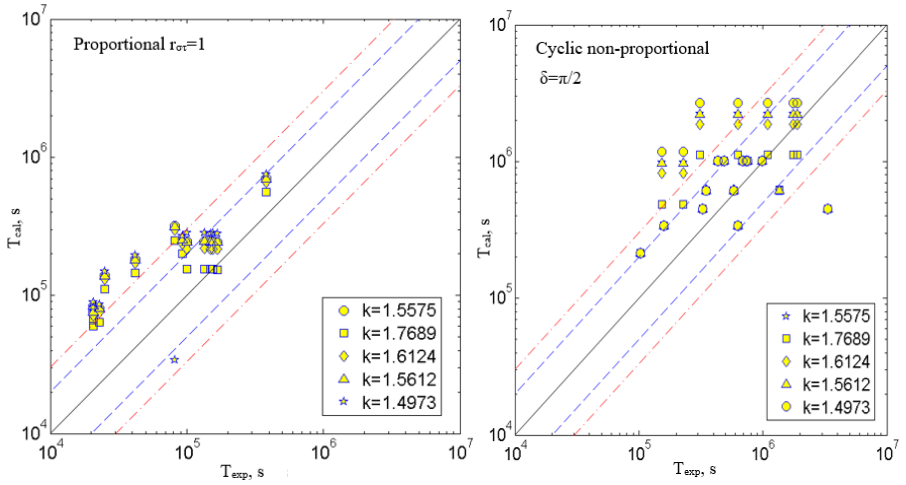

Figure 8 Comparison between experimental T_{exp} and calculated T_{cal} fatigue life for random and cyclic non-proportional with phase shift $\delta = \pi/2$ loadings

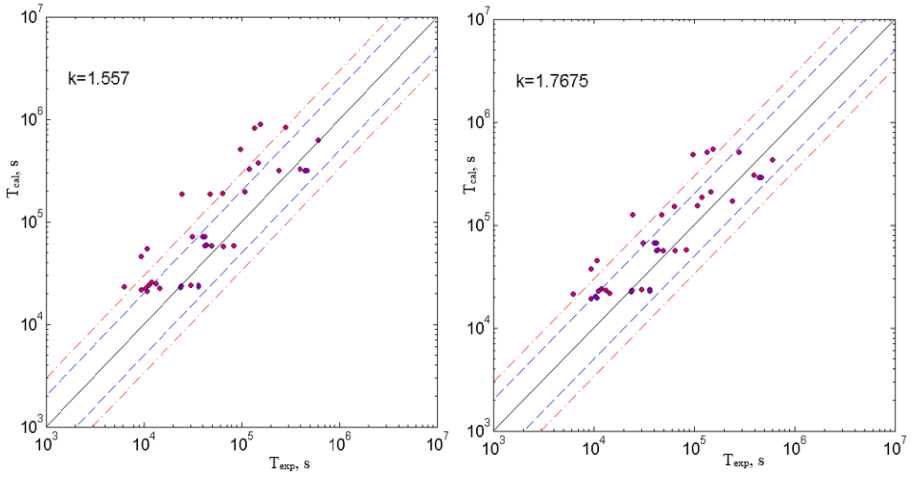

Figure 9 Comparison between experimental T_{exp} and calculated T_{cal} fatigue life for quasi-cyclic loadings

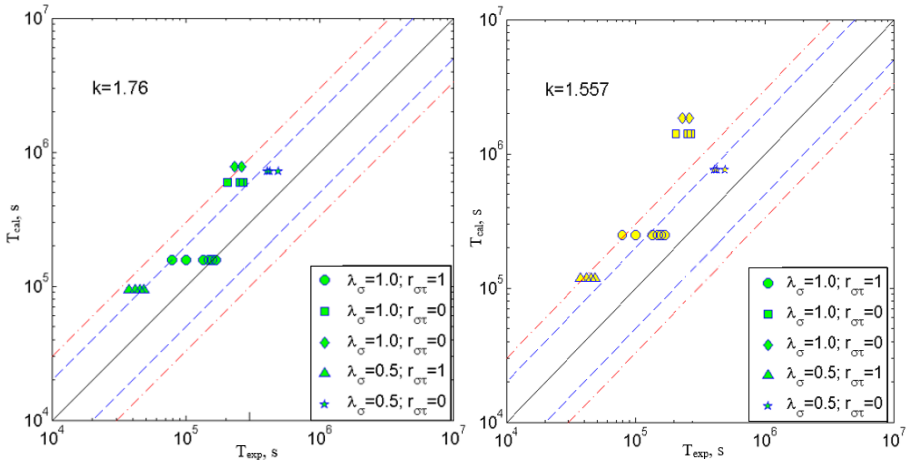

Figure 10 Comparison between experimental T_{exp} and calculated T_{cal} fatigue life for variable amplitude loadings

Figs. 11–13 present analysis of the selected results, in the form of bar graphs, which contain the percentage distribution ratios calculated fatigue life to the experimental one.

4.1. *Comparison between experimental and calculated fatigue life*

In this section summarizes the comparison between experimental and calculated fatigue life shown in Figs.7-10. For random and cyclic non-proportional with phase shift $\delta = \pi/2$ compared the results for all five values k. However, for quasi-cyclic and variable amplitude loadings made statements for the two values of k = 1.7675 – $1{\cdot}10^5$ cycles; k = 1.5575 – for fatigue limit. The graphs indicated the blue line scatter band about a factor of two, and the red line scatter band about a factor of three.

4.2. *Analysis of the results*

In section 4.2. analizing the comparison between experimental and calculated fatigue life shown on Figs.7–10. Figs. 11–13 present analysis of the results, in the form of bar graphs, which contains the percentage distribution ratios calculated fatigue life to the experimental one T_{cal}/T_{exp}, or oposite ratios T_{exp}/T_{cal} if $T_{cal} < 1$. In dark blue marked conservative results (for $T_{exp}/T_{cal} > 1$), and scatter band equal to 2. In light blue marked non-conservative results, (for $T_{exp}/T_{cal} < 1$), and scatter band equal to 2. In yellow marked conservative results, for scatter band equal to 3. In red marked non-conservative results, for scatter band equal to 3. For random and cyclic non-proportional with phase shift $\delta = \pi/2$ compared the results for three values of k = 1.4973; 1.5575; 1.7675, which are shown in the column starting from left side of drawings. For quasi-cyclic and variable amplitude loadings the analyze reduced to two values of $k = 1.5575; 1.7675$.

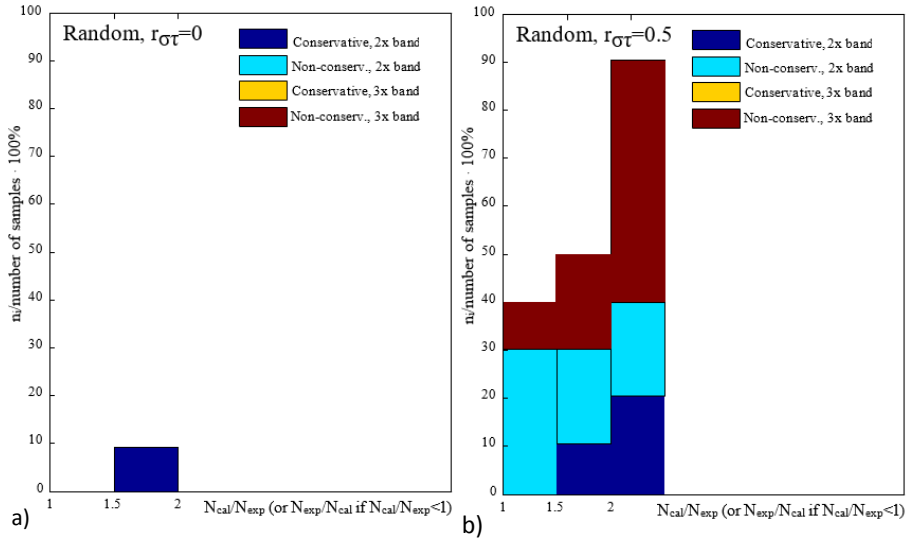

Figure 11 Analysis of the results of experimental and calculated fatigue life for random loadings and cross-correlation coefficient between normal stresses and shear stresses a) $r_{\sigma\tau} = 0$, b) $r_{\sigma\tau} = 0.5$

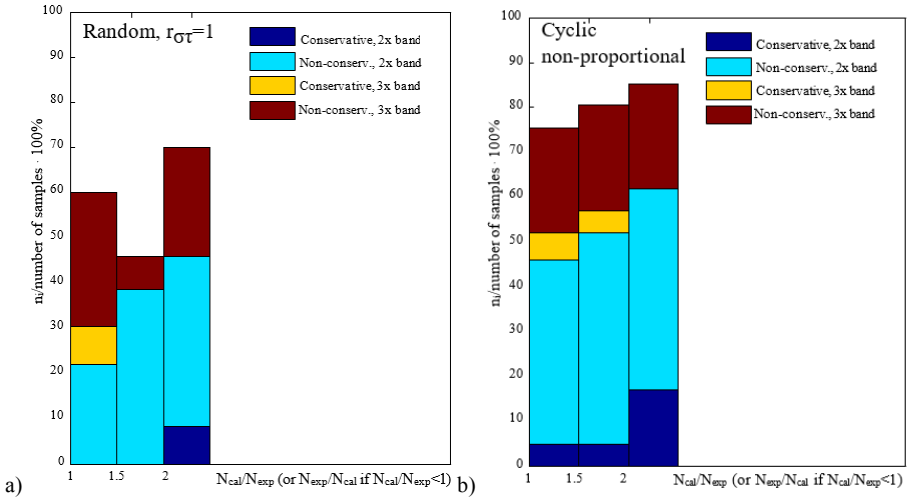

Figure 12 Analysis of the results of experimental and calculated fatigue life for a) random loadings and cross-correlation coefficient between normal stresses and shear stresses $r_{\sigma\tau} = 1$, b) cyclic non-proportional, $\delta = \pi/2$

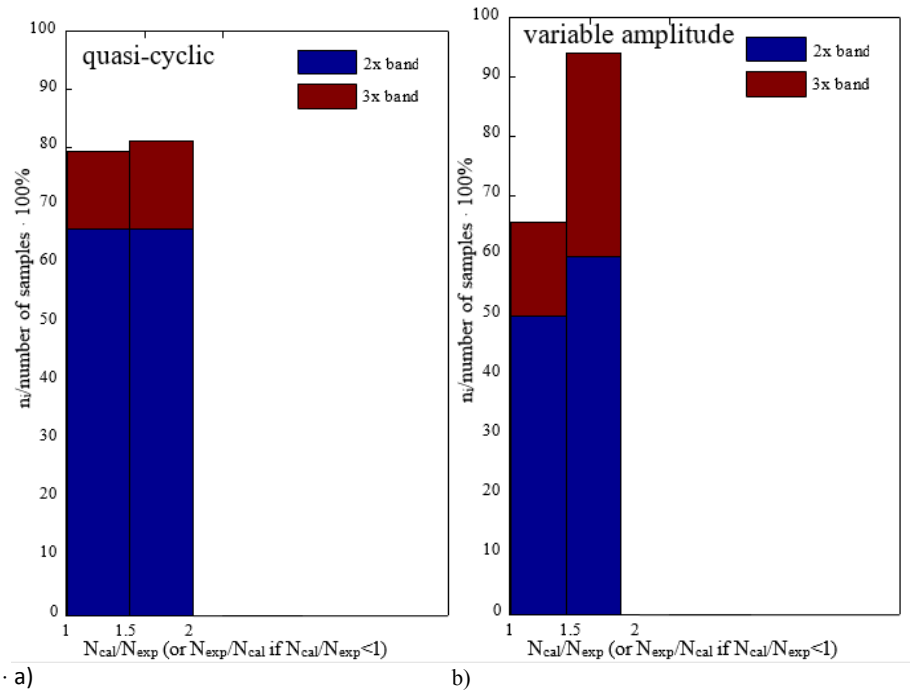

· a) b)

Figure 13 Analysis of the of experimental and calculated fatigue life for a) quasi-cyclic, b) variable amplitude loadings

k = 1.5575 – for fatigue limit,

- Random loading:

  - $r_{\sigma\tau} = 0$ – 9% results are within the 2x band;

  - $r_{\sigma\tau} = 0.5$ – 30% results are within the 2x band;,

  50% results are within the 3x band;

  - $r_{\sigma\tau} = 1$ – 30% results are within the 2x band,

  54% results are within the 3x band;

- Cyclic non-proportional:

  – 57% results are within the 2x band,

  80% results are within the 3x band;

- Quasi-cyclic:

  – 79% results are within the 2x band,

  – 66% results are within the 3x band;

- Variable amplitude:
  – 50% results are within the 2x band,
  – 61% results are within the 3x band.

For k = 1.7675 - 10^5 cycles

- Random loading:
  - $r_{\sigma\tau} = 0$ – 9% results are within the 2x band;
  - $r_{\sigma\tau} = 0.5$ – 40% results are within the 2x band,
  70% results are within the 3x band;
  - $r_{\sigma\tau} = 1$ – 46% results are within the 2x band,
  73% results are within the 3x band;
- Cyclic non-proportional:
  – 62% results are within the 2x band,
  86% results are within the 3x band;
- Quasi-cyclic:
  – 67% results are within the 2x band,
  82% results are within the 3x band;
- Variable amplitude:
  – 66% results are within the 2x band,
  94% results are within the 3x band.

5. Conclusions

In any analyzed case of loading, and for all cross-correlation coefficient between normal stresses and shear stresses $r_{\sigma\tau}$, 95% of the calculated fatigue life T_{cal} is located in non-conservative zone, or within the 2x band. For cyclic non-proportional loadings with phase difference between applied torsion and bending $\delta = \pi/2$, 90% of the results are located in non-conservative side, while for proportional loadings ca. 90% results are located in conservative side. For random loading, and cross-correlation coefficient between normal stresses and shear stresses $r_{\sigma\tau} = 0$ more than 95% results are located above 3x band, while the rest cases ca. 20% T_{cal} exceeds 3x band.

1. The proposed by Gaier and Danbauer form of the algorithm is not suited for random loadings with zero cross-correlation coefficient. In the rest of the cases of cross-correlation coefficients ca. 50% results are within the 3x band.
2. For cyclic non-proportional, quasi-cyclic and variable amplitude loadings ca. 80% results are within the 3x band.
3. For all combinations of loadings most of the results is located in non-conservative side.

References

[1] **Karolczuk A., Kluger K., Łagoda T.**: A correction in the algorithm of fatigue life calculation based on the critical plane approach. *Int. J. Fatigue*, **2016**;83:174–83, http://dx.doi.org/10.1016/j.ijfatigue.2015.10.011.

[2] **Brunbauer J., Gaier C., Pinter G.**: Computational fatigue life prediction of continuously fibre reinforced multiaxial composites, *Compos., Part B*, 80:269-277, http://dx.doi.org/10.1016/j.compositesb.2015.06.002, **2015**.

[3] **Karolczuk, A.**: Analysis of revised fatigue life calculation algorithm under proportional and non-proportional loading with constant amplitude, *Int. J. Fatigue*, 88. http://dx.doi.org/ 10.1016/j.ijfatigue.2016.03.027, **2016**.

[4] **Li, J., Li, C., Qiao, Y., Zhang, Z.**: Fatigue life prediction for some metallic materials under constant amplitude multiaxial loading. *Int. J. Fatigue*, 68, 10–23, http://dx.doi.org/10.1016/j.ijfatigue.2014.06.009, **2014**.

[5] ASTM E1049 - 85(2011)e1 Standard Practices for Cycle Counting in Fatigue Analysis, DOI: 10.1520/E1049-85R11E01

[6] **Stanfield, G.**: Discussion on: The strength of metals under combined alternating stresses, by H. Gough and H. Pollard. *Proc. Inst. Mech. Eng.*, 131, **1935**.

[7] **Gough H. J., Pollard, H. V.**: The strength of metals under combined alternating stress, *Proc. Inst. Mech. Eng.*, 131, 3–18, **1935**.

[8] **Golos, K. M., Debski, D. K., Dębski, M. A.**: A stress-based fatigue criterion to assess high-cycle fatigue under in-phase multiaxial loading conditions. *Theor Appl Fract Mech*, 73, 3–8, http://dx.doi.org/10.1016/j.tafmec.2014.07.005 **2014**.

[9] **Kulesa, A., Kurek, A., Łagoda, T., Achtelik, H., Kluger, K.**: Low Cycle Fatigue of Steel in Strain Controled Cyclic Bending. *Acta Mechanica et Automatica*, 10, 1, 62–65, doi:10.1515/ama-2016-0011, **2016**.

[10] **Kluger, K., Łagoda, T.**: New energy model for fatigue life determination under multiaxial loading with different mean values, *Int J Fatigue*, 66, 229–245, http://dx.doi.org/10.1016/j.ijfatigue.2014.04.008, **2014**.

[11] **Macha, E., Sonsino, C. M.**: Energy criteria of multiaxial fatigue failure. *Fatigue Fract Eng Mater Struct*, 22, 12, 1053–1070, doi:10.1046/j.1460-2695.1999.00220.x, **1999**.

[12] **Macek, W., Macha, E.**: The control system based on FPGA technology for fatigue test stand MZGS-100 PL, *Archive of Mechanical Engineering*, LXII, 85–100, **2015**.

[13] **Karolczuk, A., Macha, E.**: A review of critical plane orientations in multiaxial fatigue failure criteria of metallic materials, *Int J Fract*, 134, 267–304, http://dx.doi.org/10.1007/s10704-005-1088-2, **2005**.

[14] **Karolczuk, A., Macha, E.**: Płaszczyzny krytyczne w modelach wieloosiowego zmęczenia materiałów. Wieloosiowe zmęczenie losowe elementów maszyn i konstrukcji – część VI, *Studia i Monografie, issue 162*, Politechnika Opolska, Opole, 256, **2004**.

[15] **Susmel, L., Tovo, R., Socie, D. F.**: Estimating the orientation of Stage I crack paths through the direction of maximum variance of the resolved shear stress. *Int J Fatigue*, 58, 94–101, http://dx.doi.org/10.1016/j.ijfatigue.2013.05.007, **2014**.

[16] **Carpinteri, A., Ronchei, C., Spagnoli, A., Vantadori, S.**: On the use of the Prismatic Hull method in a critical plane-based multiaxial fatigue criterion. *Int J Fatigue*, 68, 159–67, http://dx.doi.org/10.1016/j.ijfatigue.2014.05.007, **2014**.

[17] **Marciniak, Z., Rozumek, D.**: Porównanie trwałości materiałów konstrukcyjnych przy obciążeniach proporcjonalnych i nieproporcjonalnych, Prace Naukowe Politechniki Warszawskiej, *Mechanika, issue 217*, Warsaw, 85–90 **2007**.

[18] **Gaier, C., Dannbauer, H.**: A multiaxial fatigue analysis method for ductile, semi-ductile, and brittle materials, *The Arabian Journal for Science and Engineering*, 33, 1B. **2008**.

[19] **Gaier, C., Dannbauer, H.**: An efficient critical plane method for ductile, semi-ductile and brittle materials, *9th International Fatigue Congress (IFC)* Atlanta **2006**.

[20] **Ince, A. Glinka, G.**: A generalized fatigue damage parameter for multiaxial fatigue life prediction under proportional and non-proportional loadings, *Int J Fatigue*, 62:34–41. http://dx.doi.org/10.1016/j.ijfatigue.2013.10.007, **2014**.

[21] **Skibicki, D.**: Multiaxial fatigue life and strength criteria for non-proportional loading, —textitMP Met., 48, 99–102, **2006**.

[22] **Skibicki, D., Pejkowski, Ł.**: Integral fatigue criteria evaluation for life estimation under uniaxial combined proportional and non-proportional loadings, *J. Theor. Appl. Mech.*, 50, 1073–86, **2012**.

[23] **Lee, S. B.**: A criterion for fully reversed out-of-phase torsion and bending. Multiaxial fatigue ASTM STP 853. Philadelphia: ASTM International, **1985**.

[24] **Macek, W., Macha, E.**: Energy-saving Mechatronic System for Fatigue Tests of Materials under Variable-amplitude Proportional Bending and Torsion, *Solid State Phenomena*, 164, 67–72, **2010**.

[25] **Findley, W. N., Coleman, J. J., Hanley, B. C.**: Theory for combined bending and torsion fatigue with data for SAE 4340 steel, *Proc. Int. Conf. on Fatigue of Metals*, London, 150–157, **1956**.

[26] **Pawliczek, R., Prazmowski, M.**: Study on material property changes of mild steel S355 caused by block loads with varying mean stress International Journal of Fatigue 80, 171–177, **2015**.

[27] ASTM E739-91. Standard practice for statistical analysis of linear or linearized stress-life (S–N) and strain-life (e–N) fatigue data. West Conshohocken, PA: ASTM Int., 553–68, **1998**.